New Journal of Physics
The open access journal at the forefront of physics

Deutsche Physikalische Gesellschaft DPG
IOP Institute of Physics

Published in partnership with: Deutsche Physikalische Gesellschaft and the Institute of Physics

OPEN ACCESS

RECEIVED
4 January 2022

REVISED
9 May 2022

ACCEPTED FOR PUBLICATION
17 May 2022

PUBLISHED
1 June 2022



PAPER

# Anderson localization in the Anderson–Hubbard model with site-dependent interactions

T H Y Nguyen[1,2], D A Le[3] and A T Hoang[1,2,*]

[1] Graduate University of Science and Technology, Vietnam Academy of Science and Technology, 18 Hoang Quoc Viet, Hanoi, Vietnam
[2] Institute of Physics, Vietnam Academy of Science and Technology, 10 Dao Tan, Hanoi, Vietnam
[3] Faculty of Physics, Hanoi University of Education, 136 Xuan Thuy, Hanoi, Vietnam
[*] Author to whom any correspondence should be addressed.

**E-mail:** hatuan@iop.vast.vn

**Keywords:** Anderson–Hubbard model, Anderson localization, site-dependent interactions, typical medium theory

Supplementary material for this article is available online

## Abstract

We consider Anderson localization in the half-filled Anderson–Hubbard model in the presence of either random on-site interactions or spatially alternating interactions in the lattice. By using dynamical mean field theory with the equation of motion method as an impurity solver, we calculate the arithmetically and geometrically averaged local density of states and derive the equations determining the critical value for the phase transition between metallic, Anderson and Mott insulating phases. The nonmagnetic ground state phase diagrams are constructed numerically. We figure out that the presence of Coulomb disorder drives the system toward the Anderson localized phase that can occur even in the absence of Anderson structural disorder. For the spatially alternating interactions, we find that the metallic region is reduced and the Anderson insulator one is enlarged with increasing interaction modulation. Our obtained results are relevant to current research in ultracold atoms in disordered optical lattices where metal–insulator transition can be observed experimentally by using ultracold atom techniques.

## 1. Introduction

In optical lattices, ultracold atoms are similar to electrons in condensed matter physics in the sense that they can realize model Hamiltonians, such as the Anderson and Hubbard models. Many notable phenomena have been observed in this regard, for example the Mott transitions in system of bosons and system of fermions [1, 2] or BEC-BCS crossover [3, 4]. Ultracold atoms have significant advantages over condensed matter systems, including high controllability of interaction strength, particle number, lattice geometry, and other parameters. Typical experiments are performed in lattices without disorder. However, disorder in the laser potential can be introduced in a variety of methods, including employing an optical speckle laser or superimposing two laser beams with incompatible frequencies [5, 6]. In addition to the control of the confinement potentials, the interaction between atoms is controlled by means of Feshbach resonances [7, 8]. Furthermore, the interaction strength between atoms can be changed spatially in $Yb^{174}$ gas system [9] as well as its disorder can be generated in a controlled manner in ultracold gases on the verge of a Feshbach resonance [10, 11]. Although theoretical and practical researches on bosons in optical lattices with random on-site interactions have been done [10–12], the fermion systems with random local Coulomb repulsion, have barely been discussed so far. Recently, the disordered Hubbard model with three different disorders involving the ionic energy, the on-site interaction strength and the hopping amplitude has been proposed and the influence of each type of disorder on the thermodynamic properties of the system has been studied [13]. On the other hand, disorder always exists in real materials, but up to now, in most studies, the disorder was restricted to the random on-site potential while the Coulomb repulsion was supposed to be the same for all sites. That is hardly justified in real situations and for models with local Coulomb interactions, such as the Hubbard and/or Anderson–Hubbard models (AHMs), disorder in on-site

Coulomb interactions should also be taken into consideration when analyzing a random medium that causes Anderson localization [13–16].

In the half-filled AHM, when a local random potential is included (we will refer to it as Anderson disorder), the paramagnetic groundstate for arbitrary interaction and disorder strength consists of metallic, Mott insulator (MI) and Anderson insulator (AI) phases. In addition, the metallic phase is identified for small values of the on-site interaction $U$ and disorder strength $\Delta$, the Mott insulating state stabilizes with increasing $U$, and large $\Delta$ favors the Anderson localization [17–19]. Besides Anderson disorder, the inhomogeneity of charge distribution through background doping and unwanted charged impurities generates random electron–electron coupling strengths (we refer to it as Coulomb disorder) [13–16]. Therefore, in order to make the model more realistic, we will also consider both sources of disorder, the Anderson and Coulomb ones, randomly distributed along the lattice. As a result, we consider the electron–electron interactions to be site-dependent in our study, which means they are assumed to be random and uniformly distributed or spatially modulated interactions across the lattice. In the half-filled AHM, we study how Anderson and Coulomb disorders might jointly contribute to the metal–insulator transition (MIT). In order to solve the problem, we employ the typical medium dynamical mean-field theory (TMT-DMFT) with geometrical and arithmetical averages over the disorder configurations, which is a successful method for the MIT on a disordered lattice [17–25]. By selecting appropriate decoupling schemes, we use the equation of motion technique as an impurity solver, which is a good option for a rapid and reliable solution [26, 27].

The paper is organized as follows. The models and our theoretical method are presented in section 2. In section 3, the averaged local density of states (LDOS) and phase diagrams are derived and discussed. In the final section, we close the paper with a short summary.

## 2. Models and method

The Hamiltonian of AHM reads

$$H = -t\sum_{\langle ij\rangle\sigma}(a^{\dagger}_{i\sigma}a_{j\sigma} + \text{h.c.}) + \sum_{i\sigma}(\varepsilon_i - \mu)n_{i\sigma} + \sum_i U_i\left[n_{i\uparrow}n_{i\downarrow} - \frac{1}{2}(n_{i\uparrow} + n_{i\downarrow})\right], \tag{1}$$

where $a_{i\sigma}(a^{\dagger}_{i\sigma})$ is the annihilation (creation) operator of an electron at site $i$ with spin $\sigma$, $n_{i\sigma} = a^{\dagger}_{i\sigma}a_{i\sigma}$ and $\mu$ denote the local electron number operator and the chemical potential, respectively, $t$ is the hopping integral for nearest neighbor sites. The local energies $\varepsilon_i$ follow a box probability distribution

$$P(\varepsilon_i) = \frac{1}{\Delta}\Theta(\Delta/2 - |\varepsilon_i|), \tag{2}$$

where $\Theta$ is the Heaviside function, $\Delta$ denotes the Anderson disorder strength.

In our paper we consider two types of site-dependent Coulomb repulsion $U_i$:

(a) $U_i$ is assumed as random and uniformly distributed within the interval $[U - \delta/2;\ U + \delta/2]$, i.e.:

$$\tilde{P}(U_i) = \frac{1}{\delta}\Theta(\delta/2 - |U_i - U|), \tag{3}$$

where $U$ is the mean value of the on-site interaction, $\delta$ is the Coulomb disorder strength. Here, we only consider the repulsive interaction, $U_i \geqslant 0$, from which $U \geqslant \delta/2$.

(b) $U_i$ is spatially alternating interactions in a bipartite lattice, i.e. $U_i = U_s$ in the sublattice $s(= A, B)$.

Within the DMFT [20, 28], the Hamiltonian (1) is mapped onto an effective Anderson model as follows

$$H_{\text{imp}} = \sum_{\sigma}(\varepsilon_i - \mu)n_{i\sigma} + U_i\left[n_{i\uparrow}n_{i\downarrow} - \frac{1}{2}(n_{i\uparrow} + n_{i\downarrow})\right] + \sum_{k\sigma}\varepsilon_k c^{+}_{k\sigma}c_{k\sigma} + \sum_{k\sigma}(V_k c^{+}_{k\sigma}a_{i\sigma} + V^{*}_k a^{+}_{i\sigma}c_{k\sigma}). \tag{4}$$

Here $c_{k\sigma}$ $(c^{+}_{k\sigma})$ annihilates (creates) an auxiliary bath electron with spin $\sigma$, $V_k$ and $\varepsilon_k$ the hybridization matrix element and the dispersion relation of the bath electrons, respectively. We use the equations of motion method [22, 27, 28] as an impurity solver for the effective Anderson model (4). We restrict our study to the nonmagnetic case at half-filling, for which $\langle n_{i\uparrow}\rangle = \langle n_{i\downarrow}\rangle = \langle n_i\rangle/2$ and $\mu = 0$. By decoupling the equations of motion at second order, the impurity Green function can be approximated as follows

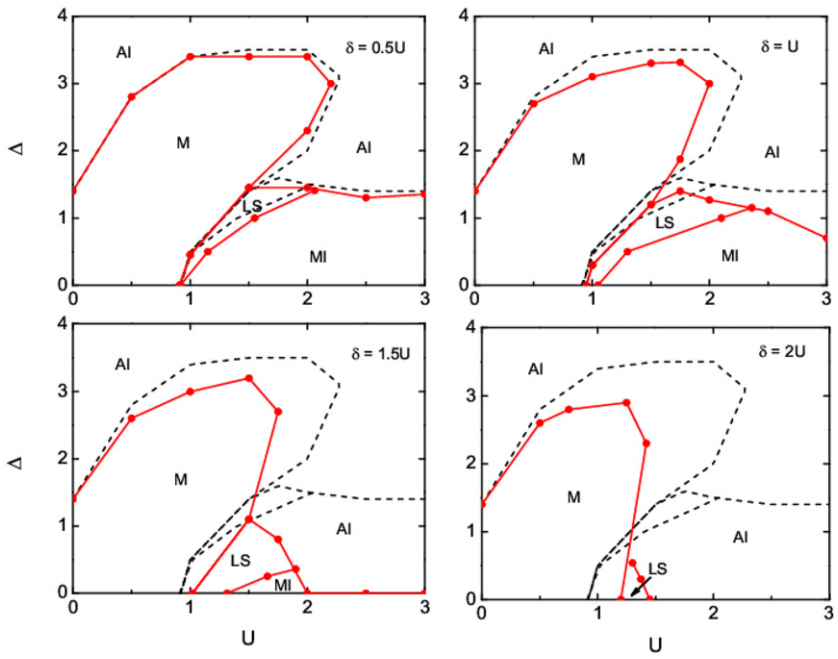


**Figure 1.** Phase diagram of the half-filled AHM for different Coulomb disorder strengths (solid line) compared with the $\delta = 0$ case (dash lines). M, AI, MI and LS stand for metal, AI, MI and localized states in the Mott gap, respectively. Energy scale: $W = 1$.

$$G(\omega, \varepsilon_i, U_i) = \frac{1 - \langle n_i \rangle/2}{\omega - \varepsilon_i + U_i/2 - \eta_i(\omega) + U_i\eta_i(\omega)[\omega - \varepsilon_i - U_i/2 - 3\eta_i(\omega)]^{-1}} + \frac{\langle n_i \rangle/2}{\omega - \varepsilon_i - U_i/2 - \eta_i(\omega) - U_i\eta_i(\omega)[\omega - \varepsilon_i + U_i/2 - 3\eta_i(\omega)]^{-1}}, \tag{5}$$

where $\eta_i(\omega)$ is the hybridization function, which describes the coupling of lattice site $i$ with all other sites of the system within the DMFT. Here, $U_i = U_s, \eta_i(\omega) = \eta_s(\omega)$ if $i \in s$-sublattice for the case of spatially alternating interactions, while $\eta_i(\omega)$ is site-independent for the case of random interactions. In the non-disorder limits, $\varepsilon_i = 0$, $U_i = U$, equation (5) is the recovery of the (full) Hubbard III approximation of the Hubbard model at half-filling [29].

For each ionic energy $\varepsilon_i$ and on-site Coulomb interaction $U_i$, the LDOS is given as

$$\rho(\omega, \varepsilon_i, U_i) = -\frac{1}{\pi} \operatorname{Im} G(\omega, \varepsilon_i, U_i). \tag{6}$$

From equation (6), one can calculate the arithmetically and geometrically averaged LDOS. We note that while the arithmetically averaged LDOS describes both extended and localized states, the geometrically one takes into account only the extended states of continuum part of the spectrum. At the Mott–Hubbard MIT, the arithmetically averaged LDOS shows an open gap at the band center whereas the geometrically one vanishes when the system is going through an Anderson transition. Thus, one can explore both types of MITs by evaluating averaged LDOS [20–24, 26].

**(i) Random on-site interactions.** The arithmetic and geometric mean of the LDOS can be evaluated by

$$\rho_{\text{arith}}(\omega) = \int \mathrm{d}U \int \mathrm{d}\varepsilon\, P(\varepsilon)\tilde{P}(U)\rho(\omega, \varepsilon, U), \tag{7}$$

$$\rho_{\text{geom}}(\omega) = \exp\left[\int \mathrm{d}U \int \mathrm{d}\varepsilon\, P(\varepsilon)\tilde{P}(U) \ln\, \rho(\omega, \varepsilon, U)\right]. \tag{8}$$

The Green function corresponding $\rho_\alpha(\omega)$, where $\alpha$ stands for either 'geom' or 'arith', is evaluated by the Hilbert transform

$$G_\alpha(\omega) = \int \mathrm{d}\,\omega' \frac{\rho_\alpha(\omega')}{\omega - \omega'}. \tag{9}$$

We use a semicircular density of states, which corresponds to an infinite-coordination Bethe lattice $\rho_0(\varepsilon) = 4\sqrt{1 - 4(\varepsilon/W)^2}/(\pi W)$ with bandwidth $W$. The self-consistent condition for the DMFT scheme is then given by

$$\eta(\omega) = W^2 G(\omega)/16. \tag{10}$$

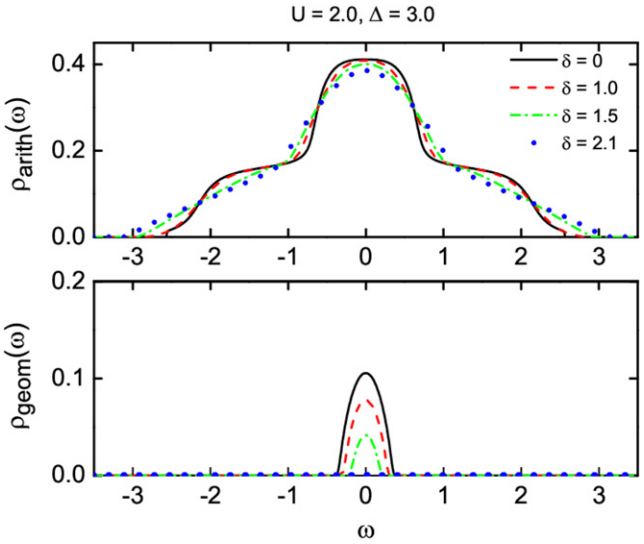


**Figure 2.** Arithmetically (geometrically) averaged LDOS with $\delta = 0, 1.0, 1.5$ and 2.1 for $U = 2.0, \Delta = 3.0$ in upper (lower) panel. Coulomb disorder drives the system from a correlated metal to the AI upon increasing $\delta$.

To numerically solve the DMFT equations (5)–(10), which allows us to get the arithmetically and geometrically averaged LDOS, the site occupation at zero temperature $\langle n_i \rangle$ is determined self-consistently as follows

$$\langle n_i \rangle = 2\int_{-\infty}^{0} \rho(\omega, \varepsilon_i, U_i)\mathrm{d}\omega. \tag{11}$$

Next, we derive the linearized DMFT equations. It is to be noticed that at the half-filling, the groundstate properties can be determined by the averaged LDOS at the band center ($\omega = 0$). In addition, the Green function at the band center is purely imaginary, $G_\alpha(0) = -\mathrm{i}\pi\rho_\alpha(0)$. Note that in the vicinity of the MIT region $\rho_\alpha(0)$ approaches zero, one can find the critical value for the phase transition from a metallic state to the Mott insulating state or to Anderson localized state by linearizing the DMFT equations [18, 22, 27]. The linearized DMFT equations with arithmetic and geometric means, which determine the boundary curves between metallic and insulating phases, are obtained as

$$1 = \frac{W^2}{16\Delta\delta}\int \mathrm{d}U \int \mathrm{d}\varepsilon\, Y(\varepsilon, U), \tag{12}$$

$$1 = \frac{W^2}{16}\exp\left[\frac{1}{\Delta\delta}\int \mathrm{d}U \int \mathrm{d}\varepsilon\, \ln\, Y(\varepsilon, U)\right], \tag{13}$$

where

$$Y(\varepsilon_i, U_i) = \frac{\varepsilon_i^2 + 3U_i^2/4 + 2\varepsilon_i U_i(1 - \langle n_i \rangle)}{[\varepsilon_i^2 - U_i^2/4]^2}. \tag{14}$$

**(ii) Spatially alternating interactions.** The arithmetically and geometrically averaged LDOS for $s$-sublattice can be now is given by

$$\rho_{s,\mathrm{arith}}(\omega) = \int \mathrm{d}\varepsilon\, P(\varepsilon)\rho(\omega, \varepsilon, U_s), \tag{15}$$

$$\rho_{s,\mathrm{geom}}(\omega) = \exp\left[\int \mathrm{d}\varepsilon\, P(\varepsilon)\ln\, \rho(\omega, \varepsilon, U_s)\right]. \tag{16}$$

The Green function for $s$-sublattice is obtained by corresponding Hilbert transform. Then using the same non-interacting DOS, the self-consistent condition now is taken the form

$$\eta_s(\omega) = W^2 G_{\bar{s}}(\omega)/16, \tag{17}$$

where $\bar{s} = B, A$ if $s = A, B$.

By an argument analogous to that used for the deriving of the linearized DMFT equations for the random on-site interactions, we get

$$1 = \frac{W^2}{16}\exp[I_{\mathrm{geom}}(U_A, U_B, \Delta)], \tag{18}$$

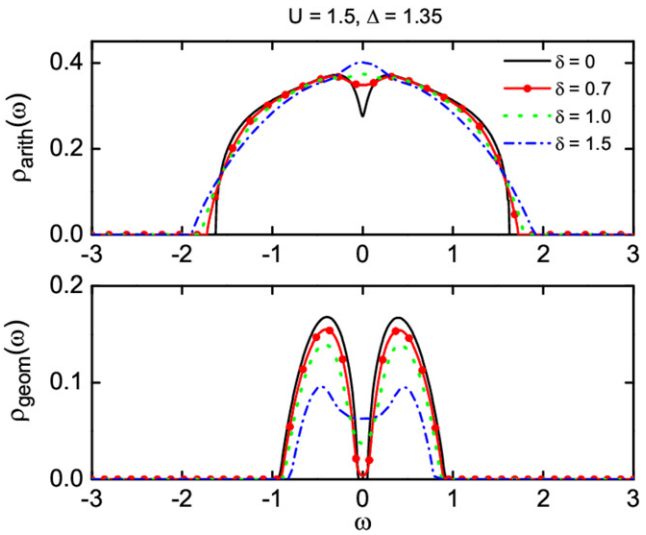


**Figure 3.** Same as in figure 2 but $U = 1.5, \Delta = 1.35$. Coulomb disorder drives the system from localized states inside the Mott gap toward the metallic phase upon increasing $\delta$.

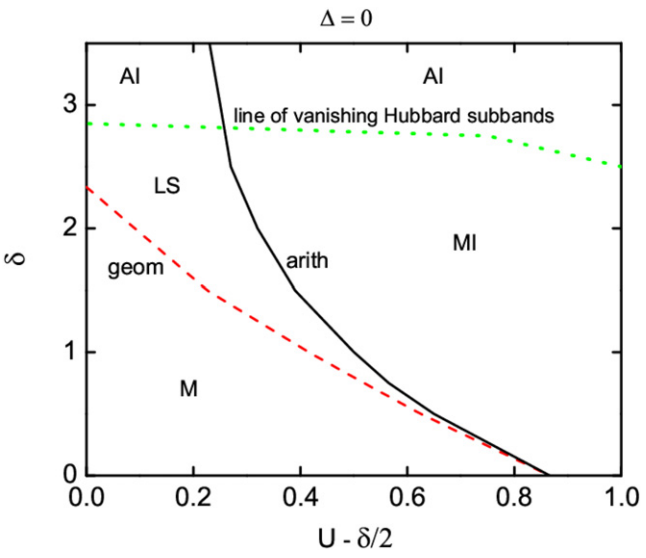


**Figure 4.** Phase diagram of the system in the absence of Anderson disorder ($\Delta = 0$) as a function of $\delta$ and $U - \delta/2$. Localized states inside the Mott gap (LS) and AI phases appear in the presence of Coulomb disorder.

where

$$I_{\text{geom}}(U_A, U_B, \Delta) = \frac{1}{2\Delta}\int \mathrm{d}\varepsilon_i \, \ln[Y_A(\varepsilon_i)Y_B(\varepsilon_i)] \tag{19}$$

for the linearized DMFT with geometric mean, and

$$1 = \frac{W^2}{16} I_{\text{arith}}(U_A, U_B, \Delta), \tag{20}$$

where

$$I_{\text{arith}}(U_A, U_B, \Delta) = \frac{1}{\Delta}\left[\int \mathrm{d}\varepsilon_i \, Y_A(\varepsilon_i) \int \mathrm{d}\varepsilon_i \, Y_B(\varepsilon_i)\right]^{1/2} \tag{21}$$

for the linearized DMFT with arithmetic mean. Here

$$Y_s(\varepsilon_i) = \frac{\varepsilon_i^2 + 3U_s^2/4 + 2\varepsilon_i U_s(1 - \langle n_i \rangle)}{[\varepsilon_i^2 - U_s^2/4]^2}, \tag{22}$$

where $\langle n_i \rangle$ is given by equation (11) with replacing $U_i$ by $U_s$.

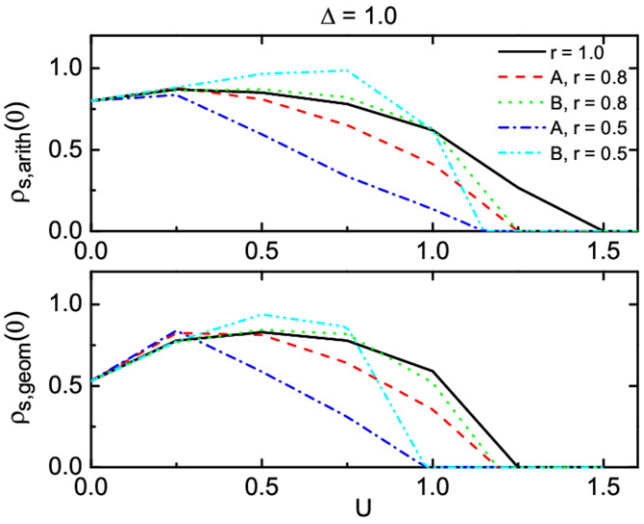


**Figure 5.** Arithmetically (geometrically) averaged LDOS in the band center $\omega = 0$ for both $s$-sublattices with $r = 1.0, 0.8, 0.5$ as a function of $U$ for $\Delta = 1.0$ in upper (lower) panel. Both $\rho_{A,\mathrm{arith}}(0), \rho_{B,\mathrm{arith}}(0)$ as well as both $\rho_{A,\mathrm{geom}}(0), \rho_{B,\mathrm{geom}}(0)$ simultaneously vanish at the critical values of $U$.

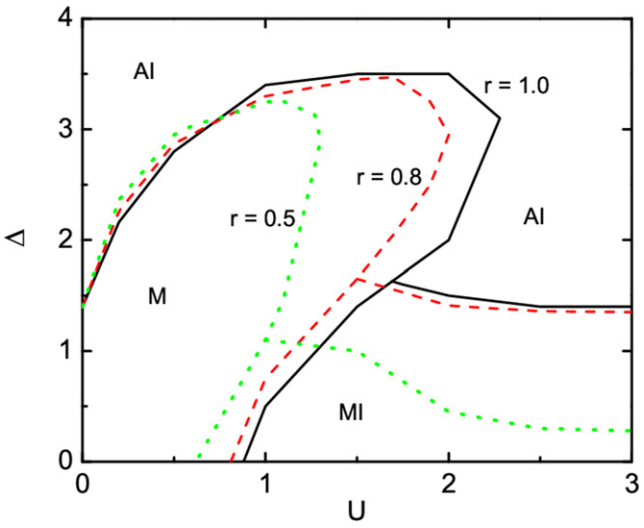


**Figure 6.** Phase diagram of the half-filled AHM with spatially alternating interactions for different values of $r = 0.5, 0.8$ compared with $r = 1$. M, AI and MI stand for metal, AI, and disordered MI, respectively.

## 3. Results and discussion

In this section, we choose $W = 1$ as the energy unit and study the phase diagrams of the system obtained from the DMFT equations presented in the previous section. The LDOS is calculated for different values of parameters in order to explore the allowed states of the system. The ground state will be investigated from the obtained values of $\rho_{\mathrm{arith}}$ and $\rho_{\mathrm{geom}}$ as follows: (1) $\rho_{\mathrm{arith}}(0) \neq 0$ and $\rho_{\mathrm{geom}}(0) \neq 0$ indicate a metallic phase; (2) $\rho_{\mathrm{arith}}(0) = 0$, $\rho_{\mathrm{geom}}(0) = 0$ and $\int \rho_{\mathrm{geom}}(\omega)\mathrm{d}\omega \neq 0$ give a Mott insulating phase; (3) $\int \rho_{\mathrm{geom}}(\omega)\mathrm{d}\omega = 0$ specifies an Anderson localized phase; (4) $\rho_{\mathrm{arith}}(0) \neq 0$, $\rho_{\mathrm{geom}}(0) = 0$ and $\int \rho_{\mathrm{geom}}(\omega)\mathrm{d}\omega \neq 0$ specify localized states inside the Mott gap. We note that the criterion of the Mott insulating phase in the Anderson–Hubbard or Anderson–Falicov–Kimball models at half-filling within TMT-DMFT studies is not exactly the same. For example, it is the quasi-particle weight drops to zero for all sites in [19]; $\rho_{\mathrm{geom}}(0) = 0$ and $\int \rho_{\mathrm{geom}}(\omega)\mathrm{d}\omega \neq 0$ in [18, 20, 23], where this is referred to as a disordered MI (gapped phase); $\rho_{\mathrm{geom}}(0) = 0$, $\int \rho_{\mathrm{geom}}(\omega)\mathrm{d}\omega \neq 0$ and $\langle n_i \rangle = 1$ for all sites in [32]. To clarify the effect of Coulomb disorder on the phase diagram, in this work we distinguish the Mott insulating phase (with a gap observed in both averaged LDOS, i.e. true Mott gap) from localized states inside the Mott gap (with a gap observed only in the geometrically averaged one) [33]. All these phases can occur for different sets of $U$, $\Delta$, and other parameters resulting in a rich phase diagram.

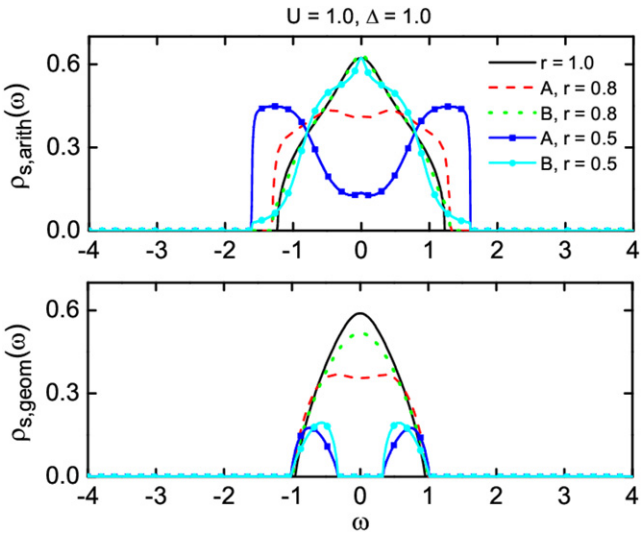


**Figure 7.** Arithmetically (geometrically) averaged LDOS for both *s*-sublattices for $\Delta = 1.0$, $U_B = 1.0$ and for different values of $r = 0.5, 0.8$ and 1.0 in upper (lower) panel. In the case of small $\Delta$ the spatial modulation interactions can enhance the localized states inside the Mott gap.

**(i) Random on-site interactions.** Figure 1 depicts the $U - \Delta$ nonmagnetic phase diagrams of the half-filled AHM for various Coulomb disorder strengths. The system can be in a metallic phase, a MI, localized states inside the Mott gap or an Anderson localization phase. It should be noted that the metallic domain and the Mott insulating domain are only connected when $\delta$ is zero. In the presence of Coulomb disorder, $\delta \neq 0$, one can see that the metallic domain and the Mott insulating domain is separated by the localized states inside the Mott gap. The extended states (metallic region) and the true band gap are no longer connected as the localized states are in between. If the Coulomb disorder increases, the metallic and Mott insulating regions shrink, whereas the Anderson localized region is enlarged. When the Coulomb disorder reaches its maximum, $\delta = 2U$, the Mott insulating region disappears, and the system enters either a metallic, Anderson localized phase or localized states inside the Mott gap. When $\delta = 2U$, the Coulomb strength $U_i$ at a given site will range from 0 to $2U$; thus, when taking the arithmetic average, there will always be a distribution from non-interacting electrons ($U_i = 0$) that prevents the establishment of a Mott insulating phase. The situation will change for all other $\delta < 2U$ values because $U_i$ at a given site will now take its value from $U - \delta/2 > 0$ to $U + \delta/2$, which dismisses the metallic state and causes the Mott gap to rise as $U$ increases. Both Anderson disorder and Coulomb disorder support Anderson localization and prevent the metallic phase as well as the MI from being established. But only Coulomb disorder can suppress the Mott insulating completely. In addition to the narrowing of the metallic and MI regions, the presence of Coulomb disorder gives rise to a new region where the system is in a localized state. That is the region where the Anderson localization is found without the Anderson structural disorder ($\Delta = 0$).

Coulomb disorder plays an important role in spectral density, as seen in figures 2 and 3 for given values of $\Delta$ and $U$. The major effect of Coulomb disorder is to drive the system to the Anderson localized phase. Firstly, the Coulomb disorder $\delta$ can drive the system from a metallic phase toward the Anderson localization when $\Delta$ and $U$ are large. In figure 2, we plot the arithmetically (geometrically) averaged LDOS for $U = 2.0, \Delta = 3.0$ in the upper (lower) panel with $\delta = 0, 1.0, 1.5$, and 2.1. One can see that with increasing $\delta$ the band length of the arithmetically (geometrically) averaged LDOS becomes larger (smaller). In addition, for small $\delta(= 0.0, 1.0, 1.5)$ both arithmetically and geometrically averaged LDOS at the band center ($\omega = 0$) are finite, which indicates a metallic state. For increasing $\delta$, the natural tendency for localization is clearly seen. For larger $\delta(= 2.1)$ the arithmetically averaged LDOS at the band center $\rho_{\rm arith}(0) > 0$ but $\int \rho_{\rm geom}(\omega)\mathrm{d}\omega = 0$ indicates Anderson localization without a Mott gap. Thus, in this case, the Coulomb disorder drives the system from a metallic phase to an Anderson localized one. Secondly, the Coulomb disorder can drive the system from localized states inside the Mott gap toward a metallic phase when $\Delta$ is small and $U$ is large. For example, when $\delta < 0.70$ ($\delta = 0$, for example), the system is in localized states inside the Mott gap because $\rho_{\rm arith}(0) \neq 0$, $\rho_{\rm geom}(0) = 0$ and $\int \rho_{\rm geom}(\omega)\mathrm{d}\omega \neq 0$, but when $\delta > 0.70$ ($\delta = 1.0, 1.5$ for examples), the system is in a metallic phase as shown in figure 3 for $U = 1.5, \Delta = 1.35$. For increasing $\delta$, there is a natural tendency for a metallic state as the gap vanishes. Therefore, in this case, the Coulomb disorder drives the system from the localized states inside the Mott gap to a metallic state.

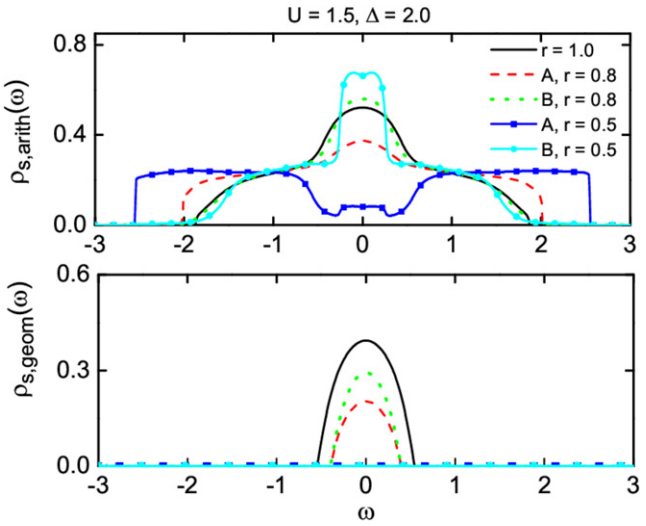


**Figure 8.** Geometrically averaged LDOS for both sublattice at $\Delta = 2.0$, $U = 1.5$. In the case of large $\Delta$ and $U$ the spatial modulation interactions can enhance the Anderson localization.

In figure 4, we present the $\delta, U - \delta/2$ phase diagram for $\Delta = 0$. It shows that at $\delta = 0$ the system contains the metallic and Mott insulating phases, but in the presence of Coulomb disorder the localized states inside the Mott gap arise. Indeed, when $\delta \neq 0$ the solutions of equations (12) and (13) do not give the same results. Increasing $\delta$ leads to a narrowing of the metal regime and a widening of the MI one. For $\delta > 2.32$ the metal region disappears, and a phase diagram with only insulator regions is obtained. In strong interaction regime, the metallic states are not available as the system is always gapped regardless of disorder strength [18, 21]. It is interesting to note that new AI regions that appear in the absence of Anderson disorder were found in the Bose–Hubbard model [10, 11] as well as in the Anderson–Falicov–Kimball with random on-site interactions [30], now we for the first time find it in the AHM with Coulomb disorder.

**(ii) Spatially alternating interactions.** Equations (18)–(22) must be numerically solved for spatially alternating interactions. In the absence of the Anderson disorder, $\Delta = 0$, from equation (20) we obtain the expression for critical interactions in the Hubbard model with spatially alternating interaction $U_A U_B = 3W^2/4$, which agrees with result in reference [31]. For the usual AHM with $U_A = U_B$ our equations (18)–(21) are reduced to equations (11)–(14) in reference [22].

In order to present our numerical results for spatially alternating interactions, we set $U_B = U$ and $r = U_B/U_A$ using the spatial modulation parameter $r : 0 \leqslant r \leqslant 1$. Figure 5 depicts arithmetically (geometrically) averaged LDOS in the band center with $\omega = 0$ for both sublattices with $r = 1.0, 0.8$, and 0.5 as a function of $U$ for fixed $\Delta = 1.0$. One can see that both $\rho_{A,\mathrm{arith}}(0), \rho_{B,\mathrm{arith}}(0)$ as well as both $\rho_{A,\mathrm{geom}}(0), \rho_{B,\mathrm{geom}}(0)$ simultaneously vanish at the phase transition. It is well established that in the Hubbard model with spatially alternating interactions both $\rho_{A,\mathrm{arith}}(0), \rho_{B,\mathrm{arith}}(0)$ simultaneously vanish at the Mott MIT [34–36]. This feature is nevertheless kept in the system in the presence of disorder, as shown above. Furthermore, both $\rho_{A,\mathrm{geom}}(0), \rho_{B,\mathrm{geom}}(0)$ also simultaneously vanish at the Anderson MIT. It means that for a fixed $r$ a single phase transition occurs in the system when the disorder and interaction strengths reach their critical values.

The nonmagnetic groundstate phase diagram, the main result of our investigation for spatially alternating interactions, is shown in figure 6 for different values of $r = 0.5, 0.8$ and 1.0. In this phase diagram we do not distinguish the Mott insulating phase from localized states inside the Mott gap one, but simply refer them to a disordered MI. Our result in the limit $r = 1$ is generally in agreement with those discovered from other TMT-DMFT [19, 22–24] and from the statistical DMFT [37]. For $0 < r < 1$ three different phases (metal, MI and AI) can be seen in the phase diagram as $r = 1$, but their regions are changed. In the case $\Delta = 0$ and fixed $U_B$, the smaller $r$ means the larger $U_A = U_B/r$ and the easier it is to localize the system. Our calculations show that this is still true for small $\Delta(\Delta < \Delta_c(U = 0) = e/2)$ and any given value of $U$, and that it is also true for large $U$ when $\Delta$ is larger. As a result, the metallic region is reduced, and the AI region is enlarged by decreasing the spatial modulation parameter $r$. It is worth noting that the MI phase is not observed in the system for any $U_A$ when $r = 0$, because there is no interaction in the $B$-sublattice. In this case, what phase (metallic or AI) the system is in depends only on the Anderson disorder $\Delta$.

To illustrate our main results, we calculate the arithmetically (geometrically) averaged LDOS for both sublattices for $\Delta = 1.0$, $U = 1.0$ and for different values of $r = 0.5, 0.8$ and 1.0 in upper (lower) panel. As can be seen from figure 7, for $r = 1$ and 0.8 the system is metal (both averaged LDOS in the band center is different from zero), while $r = 0.5$ it turns to a disordered MI phase (the arithmetically averaged LDOS in the band center is finite, the geometrically averaged one is zero and $\int \rho_{\rm geom}(\omega)\mathrm{d}\omega \neq 0$). Thus, in the case of small $\Delta$ the spatial modulation interactions enhance the gapped phase. However, for larger $\Delta$ and $U$ the spatial modulation interactions can enhance the Anderson localization as shown in figure 8, where for $\Delta = 2.0$ and $U = 1.5$ the system is in the metallic phase for $r = 1$ and 0.8, but it turns to a AI for $r = 0.5$.

## 4. Conclusions

In summary, we studied the solutions of the half-filled AHM with site-dependent local interactions. The two simplest types of site-dependent interactions considered in the presence paper are the random and uniformly distributed one and the spatially alternating one in the lattice. We found the averaged LDOS within dynamical mean field theory with the EOM as an impurity solver using arithmetic and geometric means. In the case of random and uniformly distributed interactions, we showed that Coulomb disorder has the main effect of driving the system from a metallic state to the Anderson localized phase, and the Anderson localized states appear even in the absence of Anderson structural disorder. It is worth noting that our result is obtained using the TMT-DMFT with an approximation to the equation of motion as an impurity solver. Thus, more sophisticated many body approaches need to be formulated and applied to give a better understanding of this phenomenon. We also found that, as the Coulomb disordered strengths increase, the metallic and MI regions are reduced. For the spatially alternating interactions, in the limit $r = 0$, we figured out that the system behaves like an Anderson model independent of $U_A$. The different phases (correlated metal, disordered MI, and AI) are found for $0 < r < 1$, but their regions are changed: the metallic region is reduced, while the AI region is enlarged as $r$ decreases. Our findings are relevant to current research in ultra-cold quantum gases and mixtures in optical lattices. We expect that some of our theoretical predictions will be experimentally tested in ultra-cold quantum gases and mixtures in optical lattices in the near future because now the spectral functions of ultracold atoms in disordered potentials can be measured [38].

## Acknowledgments

This research is funded by National Foundation of Science and Technology Development (NAFOSTED) under Grant No. 103.01-2020.20.

## Data availability statement

The data that support the findings of this study are available upon reasonable request from the authors.

## ORCID iDs

D A Le https://orcid.org/0000-0003-2995-9752
A T Hoang https://orcid.org/0000-0001-8498-0541

## References

[1] Anderson B P and Kasevich M A 1998 *Science* **282** 1686
[2] Cataliotti F S, Burger S, Fort C, Maddaloni P, Minardi F, Trombettoni A, Smerzi A and Inguscio M 2001 *Science* **293** 843
[3] Greiner M, Mandel O, Esslinger T, Hänsch T W and Bloch I 2002 *Nature* **415** 39
[4] Jördens R, Strohmaier N, Günter K, Moritz H and Esslinger T 2008 *Nature* **455** 204
[5] Pasienski M, McKay D, White M and DeMarco B A 2010 *Nat. Phys.* **6** 667
[6] Fallani L, Lye J E, Guarrera V, Fort C and Inguscio M 2007 *Phys. Rev. Lett.* **98** 130404
[7] Tiesinga E, Verhaar B J and Stoof H T C 1993 *Phys. Rev.* A **47** 4114
[8] Inouye S, Andrews M R, Stenger J, Miesner H-J, Stamper-Kurn D M and Ketterle W 1998 *Nature* **392** 151
[9] Yamazaki R, Taie S, Sugawa S and Takahashi Y 2010 *Phys. Rev. Lett.* **105** 050405
[10] Gimperlein H, Wessel S, Schmiedmayer J and Santos L 2005 *Phys. Rev. Lett.* **95** 170401
[11] Gimperlein H, Wessel S, Schmiedmayer J and Santos L 2006 *Appl. Phys.* B **82** 217
[12] Zang Y C, Liu W M and Hu H 2014 *Phys. Rev.* A **90** 052722
[13] Park J and Khatami E 2021 *Phys. Rev.* B **104** 165102

[14] Kim K W, Lee J S, Noh T W, Lee S R and Char K 2005 *Phys. Rev.* B **71** 125104
[15] Lombardo P, Guisiano J C and Hayn R 2008 *Physica* B **403** 3485
[16] Morong W, Muleady S R, Kimchi I, Xu W, Nandkishore R M, Rey A M and DeMarco B 2021 *Phys. Rev. Res.* **3** L012009
[17] Dobrosavljevic V, Pastor A A and Nikolic B K 2003 *Europhys. Lett.* **62** 76
[18] Byczuk K 2005 *Phys. Rev.* B **71** 205105
[19] Aguiar M C O, Dobrosavljević V, Abrahams E and Kotliar G 2009 *Phys. Rev. Lett.* **102** 156402
[20] Byczuk K, Hofstetter W and Vollhardt D 2010 *Int. J. Mod. Phys.* B **24** 1727
[21] Carvalho R D B and Gusmao M A 2013 *Phys. Rev.* B **87** 085122
[22] Hoang A-T, Nguyen T-H-Y and Le D-A 2019 *Physica* B **570** 320
[23] Byczuk K, Hofstetter W and Vollhardt D 2005 *Phys. Rev. Lett.* **94** 0564021
[24] Oliveira W S, Aguiar M C O and Dobrosavljević V 2014 *Phys. Rev.* B **89** 165138
[25] Giovanni N, Civelli M and Aguiar M C O 2021 *Phys. Rev.* B **103** 245134
[26] Feng Q 2009 Study of single impurity Anderson model and dynamical mean field theory based on equation of motion method *PhD Thesis* Goether Universitat Frankfurt, Frankfurt
[27] Hoang A-T, Nguyen T-H-Y and Le D-A 2021 *Mod. Phys. Lett.* B **35** 2150357
[28] Georges A, Kotliar G, Krauth W and Rozenberg M J 1996 *Rev. Mod. Phys.* **68** 13
[29] Hubbard J 1964 *Proc. R. Soc.* A **281** 401
[30] Carvalho R D B, Almeida G M A and Souza A M C 2014 *Eur. Phys. J.* B **87** 160
[31] Le D-A, Tran T-T-T, Hoang A-T, Nguyen T-T and Tran M-T 2018 *Physica* B **532** 204
[32] Bragança H, Aguiar M C O, Vučičević J, Tanasković D and Dobrosavljević V 2015 *Phys. Rev.* B **92** 125143
[33] Gusmao M A 2008 *Phys. Rev.* B **77** 245116
[34] Saitou T, Koga A and Yamamoto A 2013 *J. Supercond. Novel Magn.* **26** 1771
[35] Koga A, Saitou T and Yamamoto A 2013 *J. Phys. Soc. Japan* **82** 024401
[36] Hoang A-T, Nguyen T-H-Y, Tran T-T-T and Le D-A 2016 *J. Phys. Soc. Japan* **85** 104702
[37] Semmler D, Byczuk K and Hofstetter W 2011 *Phys. Rev.* B **84** 115113
[38] Volchkov V V, Pasek M, Denechaud V, Mukhtar M, Aspect A, Delande D and Josse V 2018 *Phys. Rev. Lett.* **120** 060404